Korean Journal of Remote Sensing, Vol.21, No.1, 2005, pp.83~89

Change Detection in Land-Cover Pattern Using Region Growing Segmentation and Fuzzy Classification

Sang-Hoon Lee

Department of Industrial Engineering, Kyungwon University

Abstract : This study utilized a spatial region growing segmentation and a classification using fuzzy membership vectors to detect the changes in the images observed at different dates. Consider two co-registered images of the same scene, and one image is supposed to have the class map of the scene at the observation time. The method performs the unsupervised segmentation and the fuzzy classification for the other image, and then detects the changes in the scene by examining the changes in the fuzzy membership vectors of the segmented regions in the classification procedure. The algorithm was evaluated with simulated images and then applied to a real scene of the Korean Peninsula using the KOMPSAT-1 EOC images. In the experiments, the proposed method showed a great performance for detecting changes in land-cover.

Key Words : Remote Sensing, Change Detection, Region Growing Segmentation, Fuzzy Classification.

1. Introduction

Change detection is the process of identifying differences in the state of an object or phenomenon by observing it at different times. Remote sensing data for change detection can be used based on the fact that changes must result in detectable changes in measurement or pattern. From the beginning of the remote sensing age, the ability to measure and analyze changes on the earth environment has been seen as one of the major advantages of remote sensing. For accurate change detection, many algorithms have been developed such as image differencing (Singh, 1989), principal component analysis (Buruzzone and Prieto, 2000), change vector analysis (Buruzzone and Prieto, 2002), Markov random fields (Gong, 1993), neural network (Dai and Khorram, 1998), feature extraction (Zeng *et al.*, 2002). This study proposes an effective method for detecting land-cover changes in remote sensing using a regional growing segmentation and fuzzy classification.

The spatial region growing algorithm was suggested for image segmentation in Lee (2001, 2004a). The region-growing algorithm uses the hierarchical clustering procedure, which operates the step-by-step merging of small clusters into larger ones based on similarity measures between all pairs of candidates being considered for merging. The algorithm is designed to do merging within spatial adjacency under the

Received 15 December 2004; Accepted 30 January 2005.

hierarchical constraint and finally partition the image as any number of regions which are sets of spatially contiguous pixels so that no union of adjacent regions is statistically uniform. The fuzzy classification is an EM (expected maximization) iterative approach based on mixture probability distribution (Liang *et al.*, 1992). Under the assumption of additive Gaussian image model, given an initial class map, this approach iteratively computes the fuzzy membership vectors in the E-step and the maximum likelihood estimates of class-related parameters in the M-step, and when satisfying a convergence condition, generates the optimal class map according to the fuzzy membership vectors.

Consider two co-registered images of the same scene observed at different times. One image is supposed to have the class map of the scene at the observation time. The method performs the unsupervised segmentation and the fuzzy classification for the other image, and then detects the changes in the scene using the results of fuzzy classification. The most important advantage of the proposed detection technique is that it can apply to the comparison between the images acquired from sensors of different spectral ranges and/or with different number, position, and width of spectral bands.

The algorithm was evaluated with simulated images and then applied to a real scene of the Korean Peninsula using the KOMPSAT-1 EOC images which were acquired over Yongin-Neungpyong near to Seoul Metropolitan at March, 2000. The brief descriptions of the spatial region growing segmentation and the fuzzy classification based on the segmentation results are contained in Sections 2 and 3 respectively. Section 4 presents the algorithm using region growing segmentation and fuzzy classification. Experimental results with both simulated data and remotely-sensed data are reported and discussed in Section 5. Finally, conclusions are stated in Section 6.

2. Spatial Region Growing Segmentation

One essential structural characteristic involves hierarchy of scene information. Under the constraint of the hierarchical structure, it is then possible to determine natural image segments by combining hierarchical clustering with spatial region growing. Hierarchical clustering (Anderberg, 1973) is an approach for step-by-step merging of small clusters into larger ones. Clustering algorithm utilize a similarity/dissimilarity measure that is computed between all pairs of candidates being considered for merging, a rule for selecting the pairs to be merged, and a rule for "cutting" the hierarchical tree. The computational efficiency of hierarchical clustering segmentation is mainly dependent on how to find the best pair to be merged. The closest neighbor of region j is defined as

$$\mathrm{CN}(j) = \arg\min_{k \in R_j} d(j, k)$$

where $d(j,k)$ is the dissimilarity measure between regions j and k, and R_j is the index set of regions considered to be merged with region j. The pair of regions is then defined as MCN iff $k = \mathrm{CN}(j)$ and $j = \mathrm{CN}(k)$. It is easily shown that the best pair is one of the MCNs. In Lee (2001), the search for the best pair is limited in the set of MCNs the segmentation performs to be merged among all the MCN pairs (Lee, 2001). But, this approach updates the set of MCN pairs at every iteration, and may then result in computational inefficiency for the segmentation. Another approach to find the pairs to be merged in the clustering procedure of the segmentation was suggested in Lee (2004a). This method links two adjacent regions that are a MCN pair, using "closest neighbor chain (CN-chain)." It does not require the search of the best pair and the update of the set of MCN pairs. Both the techniques use a multi-window strategy of boundary blocking operation (Lee, 1990) to alleviate the memory problem and improve the computational performance of the algorithm.

· E-step - Calculating Indicator Vectors

$$s_{km}^{(h)} = \frac{w_k^{(h)} f_k(\mathrm{X}_m \mid \theta_k^{(h)})}{\sum_k w_k^{(h)} f_k(\mathrm{X}_m \mid \theta_k^{(h)})}$$

where

$$f_k(\mathrm{X}_m \mid \theta_k^{(h)}) \propto |\Sigma_k^{(h)}|^{-\frac{N_m}{2}} \exp\left\{-\frac{1}{2}\sum_{j\in J_m}(\mathrm{x}_j - \mu_k^{(h)})'\Sigma_k^{(h)-1}(\mathrm{x}_j - \mu_k^{(h)})\right\}$$

· M-step - Computing Maximum Likelihood Estimates of W, Θ

$$w_k^{(h+1)} = \frac{1}{N}\sum_m N_m s_{km}^{(h)}$$

$$\mu_k^{(h+1)} = \frac{1}{N w_k^{(h+1)}}\sum_m s_{km}^{(h)} \sum_{j\in J_m} \mathrm{x}_j$$

$$\Sigma_k^{(h+1)} = \frac{1}{N w_k^{(h+1)}}\sum_m s_{km}^{(h)} \sum_{j\in J_m} (\mathrm{x}_j - \mu_k^{(h+1)})'(\mathrm{x}_j - \mu_k^{(h+1)})$$

where $N = \sum_m N_m$

Fig. 1. EM iterative approach with additive Gaussian assumption.

3. Fuzzy Classification

Consider a problem classifying M regions in K classes. The data set of region m, $\mathrm{X}_m = \{\mathrm{x}_j, j \in Jm\}$, where J_m is the index set of pixels in region m and x_j is the data vector of pixel j, is associated with an unobserved image class k, which is to be estimated. This association between X_m and class k can be specified completely with an unobserved indicator vectors, $s_m = \{s_{km}, k = 1, \cdots, K\}$. In ideal situation, the kth element of s_m has unit value and all the other elements are zero if region m belongs to class k. The mixture probability distribution of the complete data set $\mathrm{Z} = \{\mathrm{X}_m, s_m\}$ is then expressed as

$$F(\mathrm{Z} \mid \mathrm{W}, \Theta) = \prod_m \prod_k w_k^{s_{km}} f_k^{s_{km}}(\mathrm{X}_m \mid \theta_k)$$

where $\mathrm{W} = \{w_k\}$ represents the weights of the components $\{f_k\}$ in the mixture distribution, $\sum_k w_k = 1$, and $\Theta = \{\theta_K\}$ is the set of parameters that define the classes. The fuzzy classification procedure calculates the indicator variables $\{s_{km}\}$ in the E-step, and the likelihood of W and Θ is maximized in the M-step using $\{s_{km}\}$ estimated in the E-step. In this study, under the assumption of additive Gaussian image model, EM iterative approach computes the fuzzy vector (Lee, 2004b) as shown in Fig. 1.

4. Detection Algorithm

Consider two co-registered images of the same scene observed at different times. One image is supposed to have the class map of the scene at the observation time. The proposed detection scheme is to find the changes in the other image based on the class map. The other image is referred to as the observed image, and the class map as the reference class configuration. The changes in the observed image are detected by the following procedure:

1) Segment the observed image using the spatial region growing algorithm.

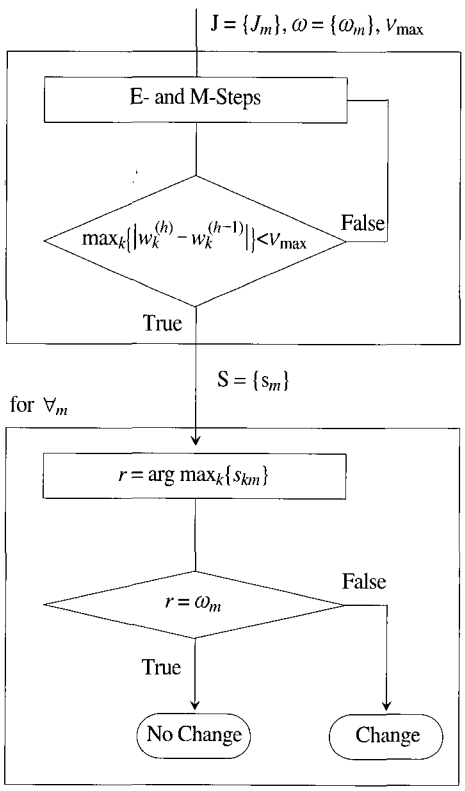

Fig. 2. Detection algorithm.

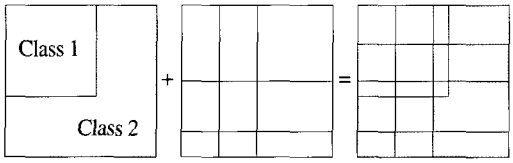

Fig. 3. Example of combining class map and region segmentation.

2) Partition the segmented regions that consist of two or more classes such that all the resultant regions have a uniform class. For example in Fig. 3, the class map has two classes and the observed image are partitioned with 9 segments, resulting in 17 segments (9 segments of class 1 and 8 segments of class 2).

3) Initialize the indicator vectors for the fuzzy classification such that the element associated with the region class of the reference configuration has unit value and all the others are zero.

4) Perform the classification and generate the final indicator vectors for the regions.

5) Detect the changes in the class configuration of the regions by comparing the initial class configuration and the resultant indicator vectors.

Fig. 3 outlines the proposed detection algorithm.

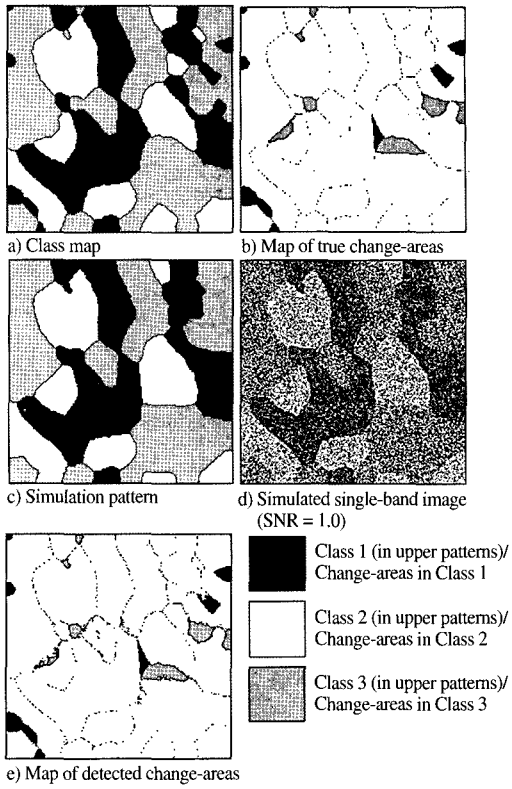

Fig. 4. Experimental data and results.

Table 1. Error Rates of Change Detection for Single-Band.

	SNR = 1.0				SNR = 2.0			
	1	2	3	Error Rate	1	2	3	Error Rate
1	306725*	1828	320	0.007	307965*	879	29	0.003
1	1037	10788	109	0.096	29	11905	0	0.002
1	35	19	14047	0.004	1	0	14100	0.000
2	18548	715	0	0.037	19103	160	0	0.008
2	6090	396390*	1844	0.020	969	402533*	822	0.004
2	4	1813	16936	0.097	0	257	18496	0.014
3	12254	199	58	0.021	12437	66	8	0.006
3	10	10389	2528	0.161	0	12807	110	0.009
3	107	1396	244397*	0.006	32	624	245244*	0.003

*: Number of pixels of the areas that were actually not changed in the original pattern and were not detected as a change area.
Underline: Number of pixels of the areas that were actually changed in the original pattern and were correctly detected as a change area

Table 2. Error Rates of Change Detection for 3 Bands

	SNR = 1.0				SNR = 2.0			
	1	2	3	Error Rate	1	2	3	Error Rate
1	308729*	81	63	0.000	308700*	159	14	0.001
1	17	11863	54	0.006	24	11910	0	0.002
1	9	1	14091	0.001	3	0	14098	0.000
2	19094	169	0	0.009	19148	115	0	0.006
2	1920	400443*	1961	0.010	1317	402068*	939	0.006
2	0	239	18514	0.013	0	110	18643	0.006
3	12453	44	14	0.005	12502	3	6	0.001
3	7	12441	469	0.037	0	12718	199	0.015
3	67	150	245683*	0.001	7	197	245696*	0.001

*: Number of pixels of the areas that were actually not changed in the original pattern and were not detected as a change area.
Underline: Number of pixels of the areas that were actually changed in the original pattern and were correctly detected as a change area

5. Experiments

Single- and 3-band 8-bit simulation images were generated using a simple pattern, which may represent a remotely-sensed environmental scene, by adding white Gaussian noise, whose variance is pixel-independent and region-dependent. Thus, the region-class process is characterized by the mean and variance of intensity values. In order to represent varying noise levels in the simulation images, the signal-to-noise ratio (SNR) is defined as the ratio of the smallest intensity-level difference to the average noise standard deviation. For computational convenience, the SNR values are the same for all bands, the variances of all region-classes are identical, and the differences between contiguous levels in order of mean intensity are constant. The proposed algorithm was first evaluated with the simulation data. This study generated simulated observation images with two levels of SNR for the single- and 3-band data respectively (1.0 and 2.0 for single band and 0.5 and 1.0 for three bands) using the additive Gaussian image model. Figs. 1-a and -b are the maps of the reference class configuration and change-areas for the experiments respectively. The pattern used to simulate the observed images and an example of simulated single-band observation with SNR = 1.0 are shown in Figs. 1-c and -d respectively. Fig. 1-e is the map of detected change-areas which results from applying the proposed detection scheme to the simulation data of Fig. 1-d. Tables 1 and 2 contain the results of the experiments for the 4 sets of simulation data. As shown in the tables, the error rates are less than 1% in almost all changes for the single-band data of SNR = 2.0 and both the 3-band data.

Next, the proposed algorithm was applied for the scene of Yongin-Neungpyung near to Seoul Metropolitan, which has been and is being briskly developed for resident and golf facilities, using the KOMPSAT-1 EOC images. Unfortunately, the EOC data set acquired over multiple years is not available to find changes in land-cover on the study area. This study has used two EOC images observed in March, 2000 with one week interval for the purpose of evaluation. The composite image was generated from them by eliminating cloud-cover and modifying bad observations such that it would be more correct to represent the target scene. Fig. 5 shows the composite image and its class map with 3 classes (Forest/Woods, Developed/ Cultivated Area, Bare Soil/Flat Area), which was

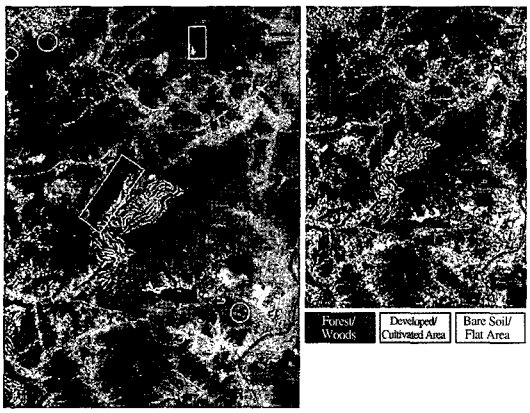

Fig. 5. Composite image (left) generated from KOMPSAT-1 EOC images observed at two different days in March, 2000 and classified map (right) with 3 classes.

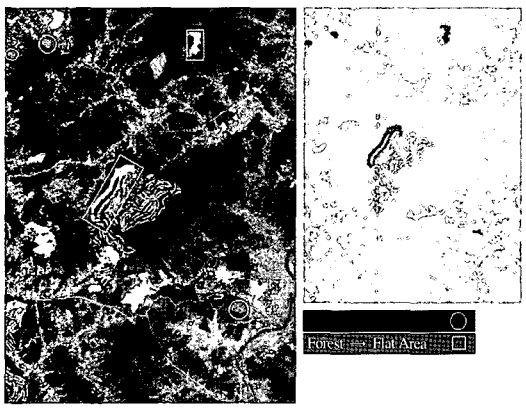

Fig. 6. Modified KOMPSAT-1 EOC image (left) of March 20, 2000 with artificial land-cover change and map of changed area (right).

produced by the unsupervised classification method of combining hierarchical clustering and fuzzy classification (Lee, 2005) and used as the reference class configuration for change detection. One of the EOC images was supposed to be the observation in this study, but there is actually no change of land-cover type in the EOC images with one-week interval. To evaluate the algorithm, this study modified the observed image by adding artificial regions such that the observed image exhibits changes in land-cover compared to the reference class configuration. Fig. 6 displays the modified observation and the map of the added artificial

Fig. 7. Map of detected changes.

regions. The forest area of 20456 pixels in the class map was assumed to change to the developed area of 3514 pixels and the flat area of 16942 pixels in the modified image. The observed data of the artificial regions were generated with additive Gaussian noise of 10 standard deviation. Fig. 7 shows the map of detected area. For the artificial regions, the proposed scheme almost perfectly detected the changes with 99.37% for the developed area and 100% for the flat area. Most of the other detected area resulted from cloud-cover and misregistration.

6. Conclusions

The most intuitive technique to detect change is simple differencing followed by threshold. Change at a pixel is detected if the difference in measurement levels of the corresponding pixels in consecutive frames exceeds a preset threshold. This technique is computationally efficient, but the result is very susceptible to noise and it is

not suitable for applications of time varying imagery. For the comparison between the images acquired from sensors of different spectral ranges and/or with different number, position, and width of spectral bands, the proposed approach, which is based on classification, is more appropriate than the conventional techniques based on the intensity values. The experimental results show that the proposed method is quite effective for the change detection in remote sensing.

References

Anderberg, M. R, 1973. *Cluster Analysis for Application*, Academic Press, NY.

Bruzzone, L. and D. F. Prieto, 2000. Automatic analysis of the difference image for unsupervised change detection, *IEEE Trans. Geosci. Remote Sensing*, 38: 1171-1182.

Bruzzone, L. and D. F. Prieto, 2002. An adaptive semi-parametric and context-based approach to unsupervised change detection in multitemporal remote sensing images *IEEE Trans. Image Processing*, 11: 452-466.

Dai, X. and S. Khorram, 1998. The effects of image misregistration on the accuracy of remotely sensed change detection, *IEEE Trans. Geosci. Remote Sensing*, 61(3): 313-320.

Gong, P., E. F. LeDrew, and J. R. Miller, 1992. Registration-noise reduction in difference images for change detection, *Int. J. Remote Sens.*, 13(4): 773-779.

Lee, S-H., 1990. *An Unsupervised Hierarchical Clustering Image Segmentation and an Adaptive Image Reconstruction System for Remote Sensing*, Ph. D. Dissertation, University of Texas at Austin.

Lee, S-H., 2001. Unsupervised image classification using spatial region growing segmentation and hierarchical clustering, *Korean Journal of Remote Sensing*, 17(1):57-70 (in Korean).

Lee, S-H., 2004a. Unsupervised image classification using region-growing segmentation based on CN-chain, *Korean Journal of Remote Sensing*, 20(3): 235-248 (in Korean).

Lee, S-H., 2004b. Fuzzy training based on segmentation using spatial region growing, *Korean Journal of Remote Sensing*, 20(5), 353-359.

Lee, S-H., 2005. Image classification based on hierarchical clustering and fuzzy membership vector, *Korean Journal of Remote Sensing*, accepted.

Liang, Z, R. J. Jaszczak and R. E. Coleman, Parameter Estimation of Finite Mixture Using the EM Algorithm and Information Criteria with Application to Medical Image Processing, *IEEE Trans. Nucl. Sci.*, Vol. 39, 1992, pp1126-1133.

Singh, A., 1989. Digital change detection techniques using remotely-sensed data, *Int J. Remote Sens.*, 10: 989-1003.

Zeng, Y., J. Zhang, and G. Wang, 2002. Change detection of guildings using high resolution remotely sensed data, *Proc. Int. Sym. Remote Sensing*, pp.530-535.